Article

Cubic Phase Content and Structure of BN Films from an X-ray Absorption Study

Xingtai Zhou, and Tsun-Kong ShamWenjun Zhang, Chit-Yiu Chan, Igor Bello, and Shui-Tong LeeHans Hofsss

Anal. Chem., **2006**, 78 (18), 6314-6319 • DOI: 10.1021/ac060160e

Anal. Chem. **2006,** *78,* 6314−6319

Cubic Phase Content and Structure of BN Films from an X-ray Absorption Study

Xingtai Zhou* and Tsun-Kong Sham

Department of Chemistry, University of Western Ontario, London, ON, Canada N6A 5B7

Wenjun Zhang,* Chit-Yiu Chan, Igor Bello, and Shui-Tong Lee

Center of Super-Diamond and Advanced Films (COSDAF) and Department of Physics and Materials Science, City University of Hong Kong, Hong Kong SAR, China

Hans Hofsäss

II. Institute of Physics, University of Göttingen, Friedrich-Hund-Platz 1, D-37077, Göttingen, Germany

X-ray absorption near-edge structure (XANES) was used to study the cubic boron nitride (c-BN) content in the BN films deposited on various substrates by different physical vapor deposition or plasma-enhanced chemical vapor deposition methods. By fitting the XANES curves of thin-film samples using standard spectra of pure c-BN and sp^2-bonded BN in the films with suitable weight factors, the c-BN contents at the film's surface region and across the film's thickness have been determined quantitatively. The results agree well with the previous transmission electron microscopic observations. The method is proved to be independent of the optical properties of thin film and provides a possibility to evaluate the cubic content of BN films accurately.

Cubic boron nitride (c-BN), as the second hardest material known so far, has been widely studied in the last two decades due to its extraordinary properties and potential applications. Cubic BN thin films have been prepared on various substrates by a number of ion-assisted physical vapor deposition (PVD) and plasma-enhanced chemical vapor deposition techniques.[1,2] The c-BN films prepared by the various ion-assisted techniques are generally a mixture of c-BN, hexagonal BN (h-BN), and amorphous BN (a-BN). Both h-BN and a-BN are sp^2-hybridized but in different structures;[1] hereafter in this paper, we use sp^2-bonded BN to represent the total of both h-BN and a-BN in thin films to simplify the discussion. The cubic phase content in the films is dependent on the preparation technique and experimental parameters.

One of the most important features characterizing the BN thin films deposited is to determine the cubic phase content. In fact, to estimate accurately the cubic phase content in the thin BN films is still a challenging work. X-ray diffraction, a conventional technique to determine the phase contents in a mixture, is generally not suitable to evaluate quantitatively the cubic phase content of c-BN film. These factors are the weakly diffracted X-ray intensity from the very thin c-BN films, the diffraction peak broadening due to the poor crystallinity of the films and the overlaps with peaks from secondary phases in the films.[1] Some other techniques, such as transmission electron microscopy (TEM)[1] and electron energy loss spectroscopy (EELS),[3−5] indeed provide some information of the cubic phase content in c-BN film in some very local positions. However, they only probe a very local spot and the results from TEM and EELS are not necessarily representative over a macroscopic film.

Until now, infrared (IR) spectroscopy has been widely used for determining quantitatively the c-BN content in BN films. For both reflection or transmission analyses, it is common to assume[1]

$$\text{volume fraction of c-BN} \sim \frac{I_{1060}}{I_{1060} + I_{1370}} \qquad (1)$$

where I_{1060} and I_{1370} are the normalized reflected or transmitted intensities of the IR absorbance at approximately 1060 and 1370 cm^{-1}, that correspond to the transverse optical (TO) modes of c-BN and h-BN, respectively. It has been realized that the c-BN content estimated from eq 1 deviates the real value for the following reasons: the film structure (the reflection of IR at interfaces in the layered structure), the optical constants of the film and the substrates, and the dependence of IR absorption on the c-BN and h-BN crystallinity.[1,6−10]

* To whom correspondence should be addressed. E-mail: xzhou44@uwo.ca and apwjzh@cityu.edu.hk.

(1) Mirkarimi, P. N.; McCarty, K. F.; Medlin, D. L. *Mater. Sci. Eng. R* **1997**, *21*, 47−100 and references therein.
(2) Zhang, W. J.; Bello, I.; Lifshitz, Y.; Lee, S. T. *MRS Bull.* **2003**, *28*, 184−188 and references therein.
(3) Golberg, D.; Bando, Y.; Eremets, M.; Kurashima, K.; Tamiya, T.; Takemura, K.; Yusa, H. *J. Electron Microsc.* **1997**, *46*, 281−292.
(4) Terauchi, M.; Tanaka, M.; Matsumoto, T.; Saito, Y. *J. Electron Microsc.* **1998**, *47*, 319−324.
(5) Li, Q.; Marks, L. D.; Lifshitz, Y.; Lee, S. T.; Bello, I. *Phys. Rev. B* **2002**, *65*, 045415.
(6) Friedmann, T. A.; Mirkarimi, P. B.; Medlin, D. L.; McCarty, K. F.; Klaus, E. J.; Boehme, D. R.; Johnsen, H. A.; Mills, M. J.; Ottesen, D. K.; Barbour, J. C. *J. Appl. Phys.* **1994**, *76*, 3088−3101.
(7) Mirkarimi, P. B.; McCarty, K. F.; Cardinale, G. F.; Medlin, D. L.; Ottesen, D. K.; Johnsen, H. A. *J. Vac. Sci. Technol., A* **1996**, *14*, 251−255.

10.1021/ac060160e CCC: $33.50
Published on Web 08/12/2006

X-ray absorption near-edge structure (XANES), a nondestructive characterization technique, measures the absorption coefficient associated with dipole transitions from core to unoccupied bound and quasi-bound states of the atoms of interest in a chemical environment. The mass absorption coefficient of a substance near its absorption edges is mainly dependent on its electronic structure and chemical environment. The crystallite size and the crystallinity have little effect on the mass absorption coefficient, so the nanocrystalline c-BN films show XANES similar to that of highly crystalline c-BN.[11−17] For BN thin films, their soft X-ray refractive index of a substance consisting of light elements, such as B and N, is very close to 1. The reflection of the soft X-ray at various interfaces in a thin-film sample is negligible as compared to that of IR light. Further, the c-BN phase ratio at the surface region and across the film thickness can be evaluated separately by choosing a different mode in the XANES measurements, i.e., the surface-sensitive total electron yield (TEY, probing depth: ~5 nm for boron and nitrogen K-edge Auger electrons) or more bulk-sensitive fluorescence yield (FY, probing depth: ~hundreds of nm, the attenuation length of fluorescent X-ray for boron and nitrogen). Actually, XANES has been employed to measure the cubic phase content in chemical vapor deposition (CVD) diamond[18] and GaN[19] thin films using a curve-fitting technique based on an assumption, in which the atoms in both sp^3-bonded and sp^2-bonded environments have the same X-ray absorption across section near their absorption edges.

In this paper, a series of samples prepared by mixing mechanically the commercially available c-BN (grain size, 4−8 μm) and h-BN powders (grain size, <44 μm) at various weight ratios was evaluated. Then the c-BN content and the c-BN distribution in BN films were investigated by analyzing their TEY- and FY-XANES spectra by curve fitting. Three BN films grown on different substrates and by different deposition methods including both PVD and CVD were chosen as the examples, i.e., sample A on (100) Si by mass-selected ion beam deposition (MSIBD), (B) on a diamond film-coated silicon substrate by electron cyclotron resonance microwave plasma chemical vapor deposition (ECR-MP CVD), and (C) again on Si (100) but by magnetron sputtering (MS). The deposition parameters of each film are summarized in Table 1, and other experimental details have already been published.[5,20,21] The c-BN contents estimated from Fourier transform infrared (FT-IR) spectra for the films are also shown for reference. The B K-edge XANES spectra were measured at the Canadian grasshopper beamline (beam size, 0.03 × 5 mm^2; total experimental full wave at half-maximum energy resolution near B K-edge, ~0.4 eV) and N K-edge spectra at the High-Energy Resolution Monochromate (HERMON) beamline (beam size, 0.1 × 5 mm^2; total experimental full wave at half-maximum energy resolution near N K-edge, ~0.5 eV), respectively, at the Synchrotron Radiation Center, University of Wisconsin—Madison. XANES spectra were recorded in both TEY and FY modes by using a specimen current and multichannel plate, respectively. After the correction of background, the spectra at the B K-edge and N K-edge are normalized to the absorption at the points of 212 and 425 eV, respectively. This ensures that the amplitude of the features is normalized to the total number of boron or nitrogen atoms in the X-ray beam.

Table 1. Deposition Parameters and the c-BN Contents Evaluated by FT-IR and XANES Analysis of BN Films

	sample		
	A	B	C
preparation technique	MSIBD	ECR-MPCVD	MS
substrate	Si (100)	CVD diamond (40 nm)/Si (100)	Si (100)
BN film thickness (nm)	80	200	80
ion energy/substrate bias	150 eV	−30 V	−75 V
substrate temperature (°C)	250	900	800
c-BN contents (in volume, whole film, from FT-IR)	≥ 90%	≥ 90%	~ 40%
c-BN contents (in weight, ~5-nm depth at surface, from XANES)	~96%	~88%	~10%
c-BN contents (in weight, whole film, from XANES)	~85%	~88%	<10%

Figure 1 shows the B K-edge (Figure 1a and b) and N K-edge (Figure 1c and d) XANES recorded in TEY and FY modes of the powder samples by mixing c-BN and h-BN powders at various ratios. At the B K-edge, a strong and narrow peak at 192 eV (peak 1) is prominent for pure h-BN powders, corresponding to the excitation of B 1s core-level electrons to the π^* states of h-BN phase. Peak 1 completely disappears for the pure c-BN powder sample due to the absence of the π^* state in c-BN. Two more peaks at 194.6 (peak 2) and 197.7 eV (peak 3) corresponding to the excitation of the B 1s core-level electron to the σ^* states of c-BN phase are observed in the pure c-BN sample. The peaks at 198.1 (peak 4) and 199.5 eV (peak 5) corresponding to the excitation of the B 1s core-level electrons to the σ^* states of h-BN appear in the pure h-BN sample. It is apparent that the relative intensity of peaks varies with the c-BN content in the mixture samples; e.g., peak 1 increases with decreasing cubic phase content (increases with the hexagonal phase content). In the B K-edge XANES (Figure 1a and b), the strongest c-BN-specific peak (peak 3) always overlays with peak 4 and peak 5 of h-BN. The

(8) Jäger, S.; Bewilogua, K.; Klages, C.-P. *Thin Solid Films* **1994**, *245*, 50−54.
(9) Tsuda, O.; Yamada, Y.; Fujii, T.; Yoshida, T. *J. Vac. Sci. Technol., A* **1995**, *13*, 2843−2847.
(10) Yokoyama, H.; Okamoto, M.; Osaka, Y. *Jpn. J. Appl. Phys.* **1991**, *30*, 344−348.
(11) Chaiken, A.; Terminello, L. J.; Wong, J.; Doll, G. L.; Taylor, C. A. *Appl. Phys. Lett.* **1993**, *63*, 2112−2114.
(12) Terminello, L. J.; Chaiken, A.; Lapiano-Smith, D. A.; Doll, G. L.; Sato, T. *J. Vac. Sci. Technol., A* **1994**, *12*, 2462−2466.
(13) Jimenez, I.; Jankowski, A.; Terminello, L. J.; Carlisle, J. A.; Sutherland, D. G. J.; Doll, G. L.; Mantese, J. V.; Tong, W. M.; Shuh, D. K.; Himpsel, F. J. *Appl. Phys. Lett.* **1996**, *68*, 2816−2818.
(14) Berns, D. H.; Cappelli, M. A.; Shuh, D. K. *Diamond Relat. Mater.* **1997**, *6*, 1883−1886.
(15) Jimenez, I.; Jankowski, A. F.; Terminello, L. J.; Sutherland, D. G. J.; Carlisle, J. A.; Doll, G. L.; Tong, W. M.; Shuh, D. K. *Phys. Rev. B* **1997**, *55*, 12025−12037.
(16) Widmayer, P.; Boyen, H.-G.; Ziemann, P.; Reinke P.; Oelhafen P. *Phys. Rev. B* **1999**, *59*, 5233−5241.
(17) MacNaughton, B.; Moewes, A.; Wilks, R. G.; Zhou, X. T.; Sham, T. K.; Chan, C. Y.; Zhang, W. J.; Bello, I.; Lee S. T.; Hofsäss, H. *Phys. Rev. B* **2005**, *72*, 195113.
(18) Fayette, L.; Marcus, B.; Mermonx, M.; Tourillon, G.; Laffon, K.; Parent, P.; Normand, F. Le *Phys. Rev. B* **1998**, *57*, 14123−14132.
(19) Katsikini, M.; Paloura, E. C.; Moustakas, T. D. *J. Appl. Phys.* **1998**, *83*, 1437−1445.
(20) Hofsäss, H.; Binder, H.; Klumpp, T.; Recknagel, E. *Diamond Relat. Mater.* **1994**, *3*, 137−142.
(21) Zhang, W. J.; Chan, C. Y.; Chan, K. M.; Bello, I.; Lifshitz, Y.; Lee, S. T. *Appl. Phys. A* **2003**, *76*, 953−955.

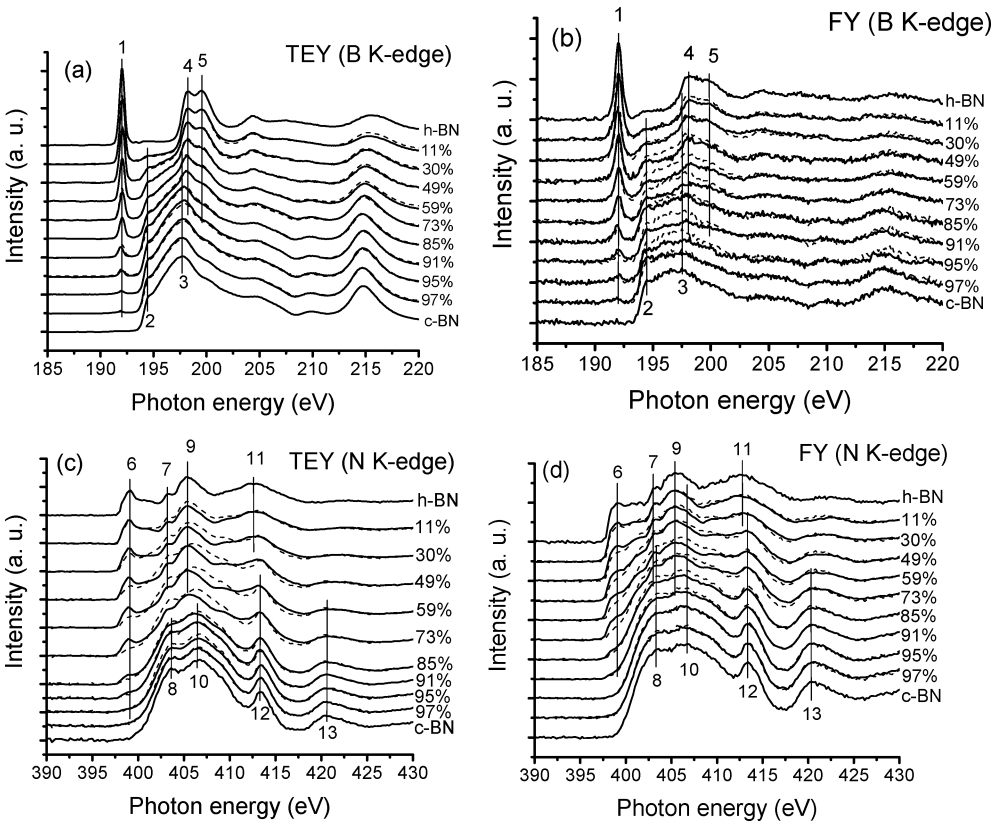

Figure 1. Measured (solid line) and calculated (dash line) B K-edge XANES recorded in TEY (a), in FY (b) and N K-edge XANES recorded in TEY (c), and in FY (d) of the mixed powder samples with various c-BN content. The values marked are the c-BN phase content (in weight) in samples or the weight factor of the c-BN phase for curve fitting.

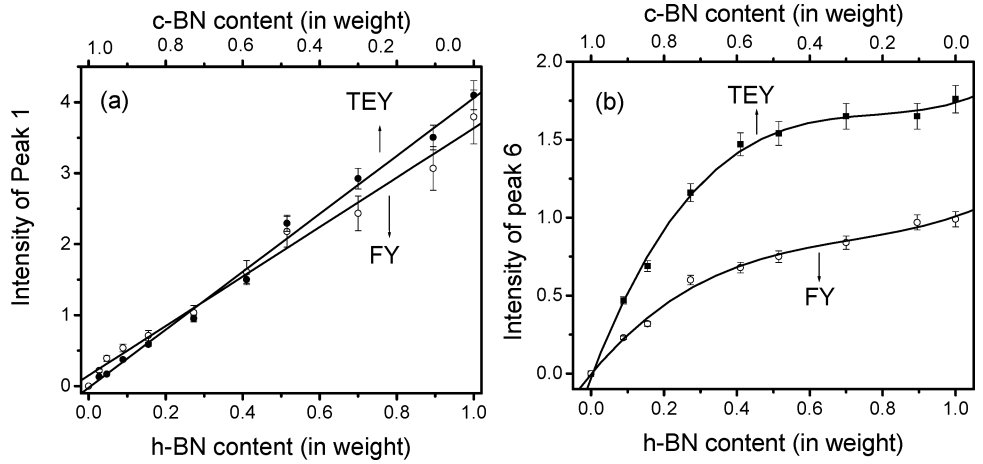

Figure 2. Dependence of the intensity of peak 1 of the XANES at the B K-edge (a) and N K-edge (b) on the h-BN phase concentration of the mixed powder sample.

intensity of peak 1 should be related to the h-BN content in the mixtures as only h-BN exhibits this 1s−π^* transition at 192 eV. The dependence of the intensity of peak 1 (relative to the edge jump) recorded in both TEY and FY on the h-BN phase content (in weight) in the mixed samples is shown in Figure 2a. Clearly, the intensity of peak 1 of both TEY and FY signals is directly proportional to the h-BN concentration (in weight) in the mixed samples. This result proves that the XANES spectra at the B K-edge of the mixed-phase BN sample can be fitted as a weighted average of the cubic and the hexagonal spectra, where the weight factors are the fractions of the coexisting cubic and hexagonal polytypes.[18,19] The calculated B K-edge XANES fitting curves (dash lines) in TEY and FY by various linear combinations of the measured XANES of the pure c-BN and h-BN powder sample with the same ratios as the mixed samples are also shown in Figure 1a and 1b, respectively. Comparing the calculated and measured spectra shown in Figure 1a and b, all measured TEY-XANES spectra match well with the corresponding calculated ones. However, the measured FY-XANES spectra do not match the corresponding calculated ones as well as the TEY-XANES spectra due to the nonuniform distribution of the phases in the mixed samples and self-absorption (thickness effect).[22,23]

(22) Meitzner, G. D.; Fischer, D. A. *Microchem. J.* **2002**, *71*, 281−286.

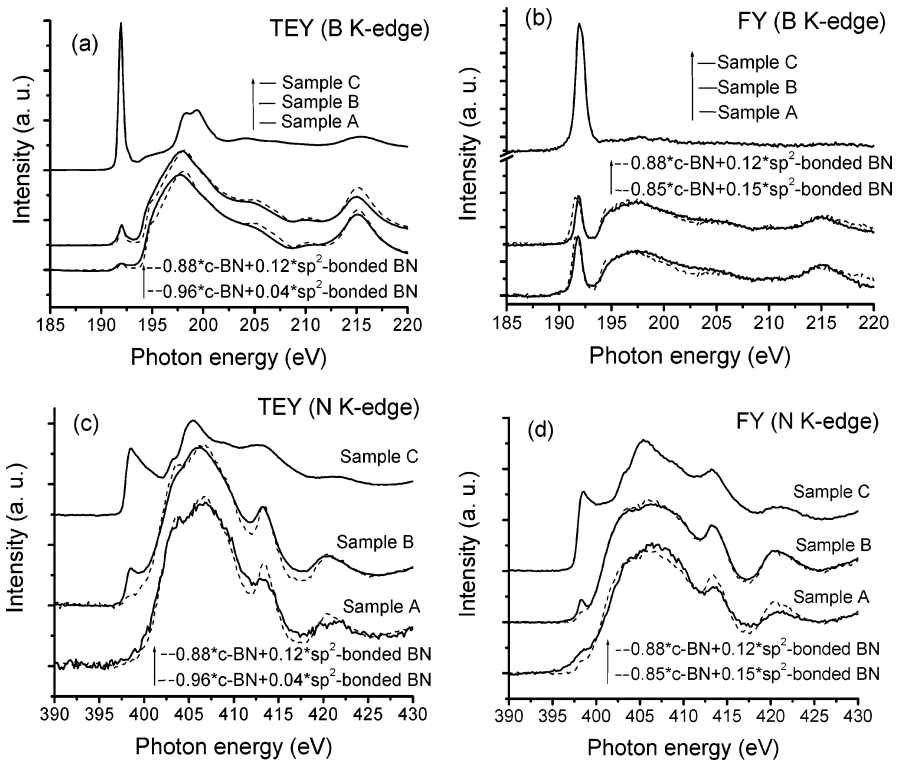

Figure 3. Measured (solid lines) B K-edge XANES recorded in TEY (a), in FY (b) and N K-edge XANES recorded in TEY (c), and in FY (d) of thin-film samples. The fitting curves (dash lines) with weights (0.96 × c-BN + 0.04 × sp^2-bond BN for sample A and 0.88 × c-BN + 0.12 × sp^2-bond BN for sample B in (a) and (c), 0.85 × c-BN + 0.15 × sp^2-bond BN for sample A and 0.88 × c-BN + 0.12 × sp^2-bond BN for sample B in (b) and (d)) are also included.

TEY (Figure 1c) and FY (Figure 1d) of the N K-edge XANES of the mixed samples are also composed of the typical c-BN and h-BN spectra although the differences in resonance features for sp^3 and sp^2 bonding are not as distinct as those in B K-edge spectra. Here, peak 6 at 399 eV corresponds to the π^* resonance of h-BN, peak 7 at 403 eV, peak 9 at 405 eV, and peak 11 at 413 eV, to the σ^* resonances of h-BN, and peak 8 at 403.5 eV, peak 10 at 407 eV, peak 12 at 413.5 eV, and peak 13 at 420 eV, to the σ^* resonances of c-BN. Their relative intensities are also dependent on the c-BN concentration. Peaks 7, 9, and 11 of h-BN phase overlay with peaks 8, 10, and 12 of c-BN phase. Similarly to the case of peak 1 at the B K-edge, the intensity of peaks 6 should also be related to the h-BN content in the mixed samples as only h-BN exhibits this π^* transition at 399 eV. It is clear that the intensity of peak 6 increases with decrease in the c-BN phase content (increases with the h-BN phase content). Figure 2b shows the dependence of the intensity of peak 6 recorded in both TEY and FY on the h-BN phase content (in weight) in the mixed samples. Unlike the case in the B K-edge spectrum, the intensity of 1s−π^* resonance (peak 6) at the N K-edge of h-BN is no longer directly proportional to the h-BN phase content in the mixed samples. When the h-BN phase content is very low (<30% in weight), the intensity of peak 6 increases more quickly with the h-BN phase content in the mixtures, but its increase with the h-BN phase content becomes slower when the h-BN phase content is higher (>30% in weight). The reason for the nonlinearity of the dependence of the intensity of peak 6 recorded in both TEY and FY on the h-BN phase concentration has not been very clear. As N is electron richer than B in the B−N bond and each N atom contributes most of the bonding electron density, N K-edge XANES of the mixed sample is probably more sensitive to the phase concentration, which results in the nonlinearity. Panels c and d in Figure 1 also show the calculated N K-edge XANES spectra (dash lines) in TEY and FY, respectively, by various linear combinations of the measured XANES of pure c-BN and h-BN powder samples with the weights, which equal the phase ratio of mixed sample. Although the intensities of peak 6 of the measured spectrum are quite different from those of the calculated spectrum, the remaining part of the spectrum, except for the part near peak 6 (397.5−401 eV), can still be nearly fitted as various linear combinations of the measured XANES of the pure c-BN and h-BN powder samples. This indicates that the phase concentration in the mixtures can still be estimated by curve fitting of the XANES at the N K-edge regardless of the mismatch of the π^* resonance of h-BN.

We now attempt to estimate the c-BN content of thin-film samples. Figure 3 shows the B K-edge XANES recorded in TEY (Figure 3a) and FY (Figure 3b), and N K-edge XANES recorded in TEY (Figure 3c) and FY (Figure 3d) of the thin-film samples A, B, and C. The c-BN phase contents (in volume for the whole film thickness) are estimated to be >90, >90, and ~40% for samples A, B, and C, respectively, by using FT-IR spectrum, as summarized in Table 1. As the film thickness is 80−200 nm, the X-ray with the energy near B and N K-edge absorption thresholds

(23) Tröger, L.; Arvanitis, D.; Baberschke, K.; Michaelis, H.; Grimm, U.; Zschech, E. *Phys. Rev. B* **1992**, *46*, 3283−3289.

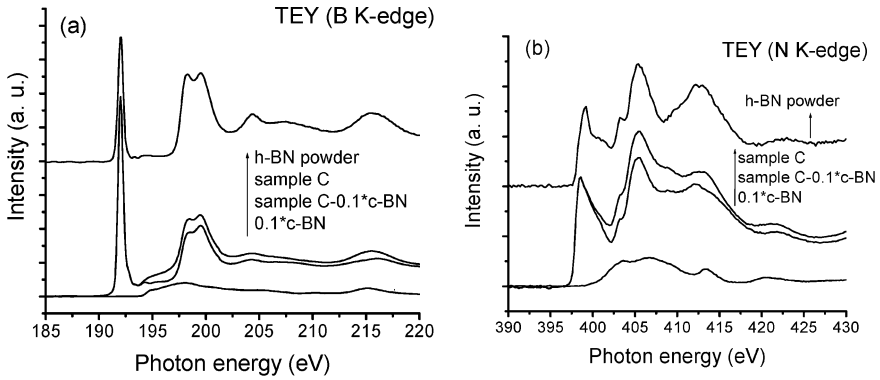

Figure 4. TEY-XANES at the B K-edge (a) and N K-edge (b) of the sp^2-bonded BN in thin-film sample C. The TEY-XANES of the pure microcrystalline h-BN powder sample are also included.

can permeate the whole film, and the c-BN content estimated from the FY signal is therefore for the whole film, while that from TEY is only for the film surface layer of ~5 nm in depth.

First let us consider the c-BN content in the surface topmost layer by analyzing the B and N K-edge spectra recorded in TEY mode. Clearly, the dominated phase in the near-surface region of samples A and B is c-BN as their TEY spectrum at both boron and nitrogen K-edge (Figure 3a and 3c) exhibits a spectrum very similar to those of pure c-BN sample together with a very weak π^* resonance (peak 1 at 192 eV at B K-edge or peak 6 at 399 eV at N K-edge). The dominated phase of sample C is sp^2-bonded BN (including h-BN and a-BN) since its TEY spectra exhibit a very strong π^* resonance (peak 1 at 192 eV at B K-edge or peak 6 at 399 eV at N K-edge). However, the sloped part in the region of 194−197 eV of the TEY of sample C shown in Figure 3a reveals that sample C contains some cubic phase BN in its near-surface region as the same part of the TEY at the B K-edge for the pure h-BN powder sample is flat (Figure 1a). The sloped part of the TEY spectrum at the B K-edge of sample C becomes flat if the TEY spectrum subtracts 10% of the TEY at the B K-edge of pure a c-BN powder sample (Figure 4a). As a reasonable approximation, we believe that sample C contains ~10% c-BN in its near-surface region and the above difference spectrum between the TEY of sample C and 10% of the TEY of the pure c-BN powder sample represents the X-ray absorption spectrum of sp^2-bonded BN at the B K-edge in the thin-film sample C. Similarly, we obtain the difference spectrum at the N K-edge between the TEY of sample C and 10% of the TEY of the pure c-BN powder sample and regard the difference spectrum as the spectrum of sp^2-bonded BN in the thin-film sample C (Figure 4b) at the N K-edge. Obviously, the TEY spectra of sp^2-bonded BN in the thin-film sample C are quite different from that of the microcrystalline h-BN. For instance, they exhibit a stronger π^* feature and some weaker σ^* features (Figure 4a and b), relative to the pure h-BN microcrystalline powder sample (Figure 1a and b). The sp^2-bonded BN with various structures in near-surface region of the thin films,[1] for example, h-BN with a grain size of nanometers or even a-BN, may exhibit XANES different from that of microcrystalline h-BN. Further, we believe that the sp^2-bonded BN in the other two thin-films, samples A and B, have similar structure and exhibit XANES spectra similar to that of sample C and the above difference spectra of sample C shown in Figure 4 were used to do the calculation of the fitting curve of the other two thin-film samples with higher c-BN phase content. Note that the difference spectra shown in Figure 4 should be renormalized when they were employed to do the curve fitting. The fitting curves (dash lines) with weights (c-BN/sp^2-bonded BN) of 0.96/0.04 and 0.88/0.12 are also shown in Figure 3a and 3c, respectively. The fitting spectra of samples A and B at the B K-edge and the fitting one of sample A at the N K-edge match very well the corresponding measured ones. The fitting one of sample B at the N K-edge, except for the π^* resonance near 399 eV, also matches well the corresponding measured one (Figure 3c). This means that samples A and B contain c-BN phase contents of ~96 and ~88% (in weight) in the near-surface region, respectively. The big difference of the π^* resonance at the N K-edge between the calculated and measured spectrum of sample B is due to the nonlinearity of the dependence of the π^* resonance intensity of the XANES at the N K-edge on the sp^2-bonded phase concentration in the thin film samples.

From the FY-XANES of the thin-film samples shown in Figure 3b and d, no noticeable signal of c-BN can be observed for sample C and c-BN phase content in the whole film of this sample should be very low (<10%). As an approximation, we regard the FY-XANES spectra of sample C shown in Figure 3b and d as the standard spectra of sp^2-bonded BN in thin films and use these spectra to do the calculation of the curve fitting for samples A and B. Similarly to the case of its TEY-XANES of the sp^2-bonded BN in thin-film sample C shown in Figure 4a and b, their π^* transition features become much stronger and their σ^* transition features weaker, compared to the FY-XANES of the pure microcrystalline h-BN powder sample (Figure 1b and d). The measured FY-XANES curves of samples A and B can also be nearly fitted as linear combinations of those of c-BN and sp^2-bonded BN in thin films with weights (c-BN/sp^2-bonded BN) of 0.85/0.15 and 0.88/0.12, respectively, which means that samples A and B contain ~85 and ~88% (in weight) in the whole film, respectively, as summarized in Table 1. Compared to the mixed powder sample with 85% c-BN (Figure 1), thin-film sample B exhibits the enhancement of π^* features (peaks 1 and 6) and the depletion of σ^* features of sp^2-bonded BN, although it contains an equivalent c-BN phase (88%) in the near-surface region or in the whole film. This results from the difference of the XANES spectrum between the sp^2-bonded BN in thin films used for curve-fitting and microcrystalline h-BN powder. Similarly, the mismatch of the intensity of the π^* resonance between the calculated and measured FY-XANES at the N K-edge of samples A and B is also due to the above mentioned nonlinearity of the dependence of the π^* resonance of the FY-XANES at the N K-edge on the sp^2-bonded

phase concentration in the thin-film sample. The comparison of the c-BN content in the whole film estimated by XANES with that by FT-IR indicates when the thin film consists mainly of c-BN phase (samples A and B); the above results by XANES are somewhat lower than those evaluated by FT-IR measurement; when the thin film is mainly composed of sp^2-bonded BN phase (sample C), the c-BN phase concentration in the whole film from FT-IR is overestimated significantly (considering the difference of phase content between in volume and in weight), as shown in Table 1. As the intensity of the XANES features is dependent on the resolution of the beamline, the cubic phase content can also be evaluated conveniently and approximately by measuring the intensity of the B K-edge XANES feature (relative to the edge-jump) if we fix the resolution of the beamline. The separation of the B K-edge XANES features between c-BN (>193 eV) and sp^2-bonded BN (peak 1 at ~192 eV) in thin-film samples (Figure 3b) and the linearity of the dependence of peak 1intensity on h-BN phase content provide this possibility.

Comparing the c-BN content in the near-surface region with the average in the whole film, sample A has a higher c-BN content at its surface (96%) but a lower one in the whole film (~85%), indicating that there may be some extra amount of sp^2-bonded BN in the depth of the film. This agrees with the existence of an a-BN and an oriented h-BN, turbostratic BN (t-BN), interlayers at the film−substrate interface as observed by TEM.[24] Sample B has equal c-BN content in the whole film and in the near-surface region (~88%), revealing that the distribution of the sp^2-bonded BN is uniform across the film thickness, which also agrees well with the fact that c-BN film grows directly on diamond film substrate without any a-BN/t-BN interlayers.[25]

Due to the involvement of energic species during their deposition, the PVD and CVD BN thin films were prepared under conditions far away from equilibrium. The structure, crystallinity, and electronic structure of the BN thin films may be quite different from those of either microcrystalline c-BN or h-BN. For instance, our experimental results show that the XANES spectra of the sp^2-bonded BN in thin films are significantly different from those of the microcrystalline h-BN powder due to the existence of a-BN, h-BN with size of nanometers,[1] or with curved graphitic layers[5] in BN thin films. However, the XANES spectra of the c-BN phase in thin films are very close to those of pure microcrystalline c-BN. The above forms of sp^2-bonded BN may have their own electronic structures. Generally, the sp^2-bonded BN in different forms coexist in thin films, which makes it hard to obtain their own particular XANES spectrum. In our analysis of the XANES results, we assume that the XANES spectra of the sp^2-bonded BN in thin films prepared with the involvement of the energic species are similar. The XANES spectra of the sp^2-bonded BN (the difference spectra shown in Figure 4) in thin=film sample C prepared by a magnetron sputtering technique are approximately used as the standard spectra of the sp^2-bonded BN in thin films for the curve fitting of the other two thin-film samples prepared by the other two techniques. Of course, the preparation technique has an effect on the electronic structure of the sp^2-bonded BN in thin films as it has effects on the structure, crystallinity, and relative concentration of the sp^2-bonded BN in different forms. The broadening of the features, difference of the XANES spectrum of the sp^2-bonded BN in thin films prepared by different techniques, and some other factors may induce the error of the cubic phase content estimated by the curve fitting of the XANES spectrum. The curve-fitting results shown in Figure 3 indicate that the above assumption and approximation are feasible. Comparing the curve-fitting results at the B and N K-edge, it is very clear that the XANES at the B K-edge are more suitable to estimate the c-BN phase content in thin films due to the more distinct resonance features and the linearity of the π^* transition intensity on the h-BN phase content for the XANES at the B K-edge.

Similarly to the IR technique, the cubic phase content estimation of thin films by XANES is also sensitive to the preferred orientation of the sp^2-bonded BN crystallites in the films because the synchrotron radiation is a polarized X-ray; the relative intensity of the h-BN features in XANES should be incident angle dependent if the sp^2-bonded BN crystallites in the thin films have a texture structure.[11,26,27] It should be noted that all above results are based on the assumption that the sp^2-bonded BN crystallites in the thin-film sample are randomly aligned. Actually, some of the sp^2-bonded BN in BN films, i.e., the t-BN at the film−substrate interface, aligns along a particular orientation,[1] and thus, there will be a deviation in the c-BN content evaluation from XANES for the thin-film samples. Further work to determine quantitatively the content of randomly aligned and oriented t-BN components in BN thin films by the angle-dependent XANES is now underway. Because of the short attenuation length of X-ray, the XANES technique is not suitable to the very thick BN film (~μm in thickness). On the other hand, as XANES is a synchrotron-based technique, its practical applicability for routine analyses is limited.

In summary, XANES was used to study the c-BN content in the BN films deposited on various substrates by PVD or CVD methods. The XANES at the B K-edge are proved to be more suitable to estimate the c-BN phase content in thin films. By using the curve fitting of the TEY- and FY-XANES, the c-BN contents at the film surface and in the whole film have been determined quantitatively and the structure of the thin films was deduced.

ACKNOWLEDGMENT

The authors acknowledge Dr. F. Heigl and Dr. A. Jürgensen at the Canadian Synchrotron Radiation Facility (CSRF) at the Synchrotron Radiation Center, University of Wisconsin−Madison, for their assistances on the XANES experiments and Dr. Y. M. Yiu for her helpful discussion. The work at the University of Western Ontario was supported NSERC and CRC (T.-K.S.). The work at the City University of Hong Kong was supported by the Research Grants Council of the Hong Kong SAR, China (Project CityU 2/04C and CityU 1131/04E).

(24) Hofsäss, H.; Ronning, C.; Griesmeier, U.; Gross, M.; Reinke, S.; Kuhr, M.; Zweck J.; Fischer, R. *Nucl. Instrum. Methods Phys. Res. B* **1995**, *106*, 153−158.

(25) Zhang, W. J.; Bello, I.; Lifshitz, Y.; Chan, K. M.; Meng, X. M.; Wu, Y.; Chan, C. Y.; and Lee, S. T. *Adv. Mater.* **2004**, *16*. 1405−1408.

(26) Zhou, X. T.; Sham, T. K.; Chan, C. Y.; Zhang, W. J.; Bello, I.; Lee, S. T.; Heigl, F.; Jürgensen, A.; Hofsäss, H. *J. Mater. Res.* **2006** *21*, 147−152.

(27) Zhou, X. T.; Sham, T. K.; Chan, C. Y.; Zhang, W. J.; Bello, I.; Lee, S. T.; Hofsäss, H. *J. Appl. Phys.* In press.

Received for review January 23, 2006. Accepted July 14, 2006.

AC060160E